Journal of
MATERIALS RESEARCH

Computer simulations of interactions between ultrafine alumina particles produced by an arc discharge

M. H. Teng, L. D. Marks, and D. L. Johnson
Department of Materials Science and Engineering, Northwestern University, 2225 N. Campus Dr., Evanston, Illinois 60208

(Received 25 September 1995; accepted 24 August 1996)

We wrote two computer programs, 3D and BUMP, to interpret transmission electron microscope (TEM) micrographs made during a study of the initial stage sintering of ultrafine alumina particles (UFP's, 20–50 nm in diameter). The first simulated the 3D geometric relationships of particles, from which we concluded that surface diffusion was the predominant sintering mechanism because no shrinkage occurred. BUMP simulated random contact of two particles and showed that the particle chains that formed before sintering were not formed purely by chance. Instead the particles experienced a rearrangement process (rotation and sliding) which reduced the total surface energy.

I. INTRODUCTION

Traditional sintering models assume spherical particle shape, and isotropic surface energy and diffusion coefficient.[1–17] The models break down when applied to submicrometer particle sizes and materials with anisotropic surface properties. To explore this new area of sintering science, a unique experiment was carried out. Ultrafine alumina particles were produced by an arc-discharge method, sintered in flight through a furnace, and collected and observed in a clean UHV environment.[18–22] The experimental results were recorded on several hundred micrographs taken by a Hitachi UHV-H9000 TEM. Although several studies related to sintering of ultrafine alumina have been reported, none was done in a well-controlled UHV environment.[23–26]

The information about the 3D arrangement of the particles was critical to the successful deduction of the sintering mechanism. Unfortunately, micrographs show only projected outlines of particles (Fig. 1). In some cases when the particles are aligned well (in a known crystal axis direction) a simple measurement of the distances between each parallel pair of outline facets would be enough and may determine their geometric center and shape.[27,28] In most cases the particles, which were in chains, were randomly oriented and their 3D relationships were impossible to determine by inspection.

Electron and x-ray diffraction revealed that the alumina particles had a spinel structure[18,20] and nearly uniform shape (see Sec. II), with only minor variations. These facts facilitated the development of simulation programs.

This paper consists of three parts. In Sec. II we define two parameters (*GR* and *V*) to describe the geometric shapes of particles. Each of the following two sections describes a simulation program that was used as a tool to solve one specific problem related to the study.

In Sec. III, the first computer program, named 3D, is described and its interactive operating procedures are briefly introduced by one example. This program helped us to find the most likely orientation and arrangement of particles observed in TEM micrographs and reduced human bias to a minimum. The program also made it possible to determine whether the sintered particle pair shrank or not, thus helping to determine the predominant sintering mechanism.

In Sec. IV, the second computer program, named BUMP, simulates the random contact conditions of two alumina particles and helps determine whether the observed nonsintered particle chains were formed purely by chance (i.e., random contact) or not. If they formed by chance only, then experimental results should be identical to simulations; if rearrangement occurred, we should be able to see differences between experimental and simulation results.

II. GEOMETRIC SHAPES OF ALUMINA PARTICLES

Since alumina is a very stable material and the particles were produced from the vapor in a clean environment, we probably can ignore re-evaporation and contamination effects and assume that the particles reached their equilibrium shape. For a particle with equilibrium shape, according to the Wulff construction, the relative distance from the origin to a facet is proportional to the surface energy of the facet[29–32]:

$$\frac{\gamma_i}{h_i} = \frac{\gamma_j}{h_j} = \cdots, \tag{1}$$

 © 1997 Materials Research Society

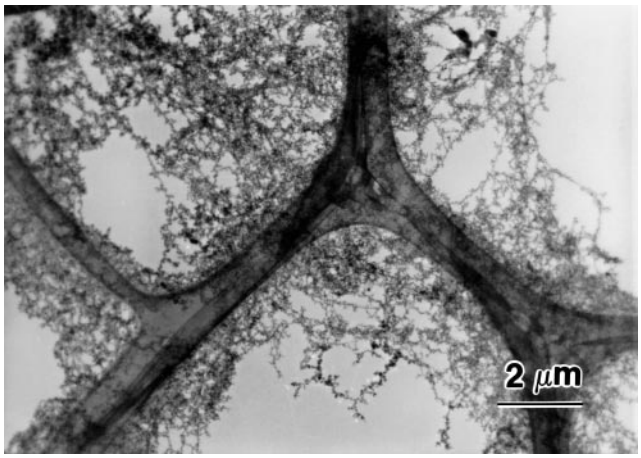

(a)

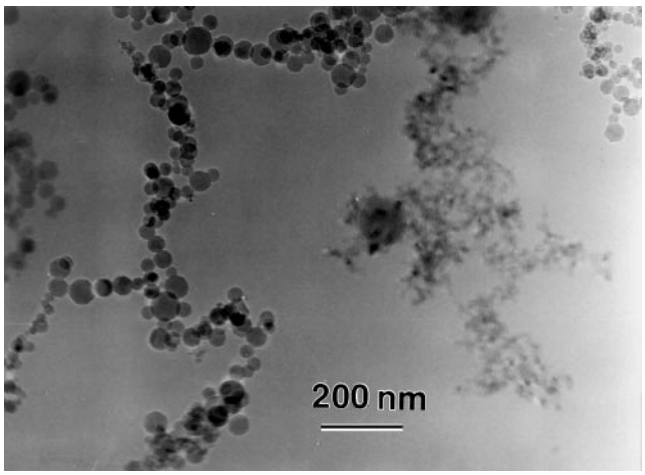

(b)

FIG. 1. (a) Low magnification view of collected (nonsintered) alumina particle chains on the grid; (b) one chain of these sintered particles.

where h_i and h_j are the distances from a common center drawn normal to crystal facets *i* and *j*, and γ_i and γ_j are the surface energies of facets *i* and *j*.

The particles are enclosed by three types of facets: {100}, {111}, and {110}. In the absence of {110} facets, then {100} and {111} define a cuboctahedron (Fig. 2). By setting the distance from the origin to {100} to be unity and varying the relative distance from the origin to {111} from 0.577 (an octahedron, only {111} exists) to 1.732 (a cube, only {100} exists), we can easily define the shape of a cuboctahedron by the parameter *GR* (energy ratio):

$$GR = \frac{\gamma_{111}}{\gamma_{100}} = \frac{h_{111}}{h_{100}}, \tag{2}$$

where γ_{111} and γ_{100} are the surface energies of {111} and {100}, and h_{111} and h_{100} are the distances from origin to facets {111} and {100}.

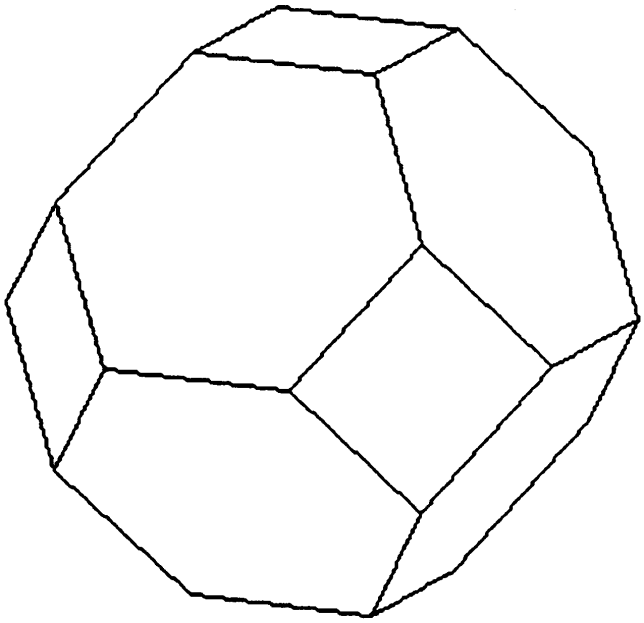

FIG. 2. A cuboctahedron particle demonstrates the definition of the shape-controlling factor *GR* (energy-ratio). *GR* is the ratio of the normal distance from the particle center to {111} over that of {100}; *GR* also represents the relative surface energy of {111} over {100} in the Wulff construction.

We could have defined another energy ratio parameter for γ_{110} vs γ_{100} and thus completed the construction of the typical shape of an alumina particle, i.e., a cuboctahedron with addition of {110}. However, since the {110} is actually a hill-and-valley structure (Fig. 3) composed of two sets of small {111} facets with 109.5° interangle, {110} are more like add-on facets.[32] In other words, the macroscopic {110} does not coincide with equilibrium shape as a flat surface; therefore, there is no physical justification to define a γ_{110} vs γ_{100} parameter. Instead it is more reasonable to define a {110} size parameter, *V*, as a function of the degree of development of {110} on a cuboctahedron:

$$V \equiv \frac{1}{2}\left(1 - \frac{L}{L_0}\right), \tag{3}$$

where *L* is the length of the intersection between {100} and {111}, and L_0 is the length when {110} does not exist; i.e., L_0 is the maximum length and the length of the edge between {100} and {111} of a cuboctahedron (Fig. 4). The size of {110} can vary from zero [Fig. 4(a)] to a maximum [Fig. 4(b)] when they impinge on each other. If there are no {110} planes, $V = 0$; when the {110} area is maximum then $V = 0.5$. The increase of {110} area is at the expense of four surrounding facets, two {111} and two {100}. Note that when the {110} facet area increases, its four corners also shift toward the center of the four intersection edges of surrounding {111} and {100} (Fig. 4). After examining hundreds of

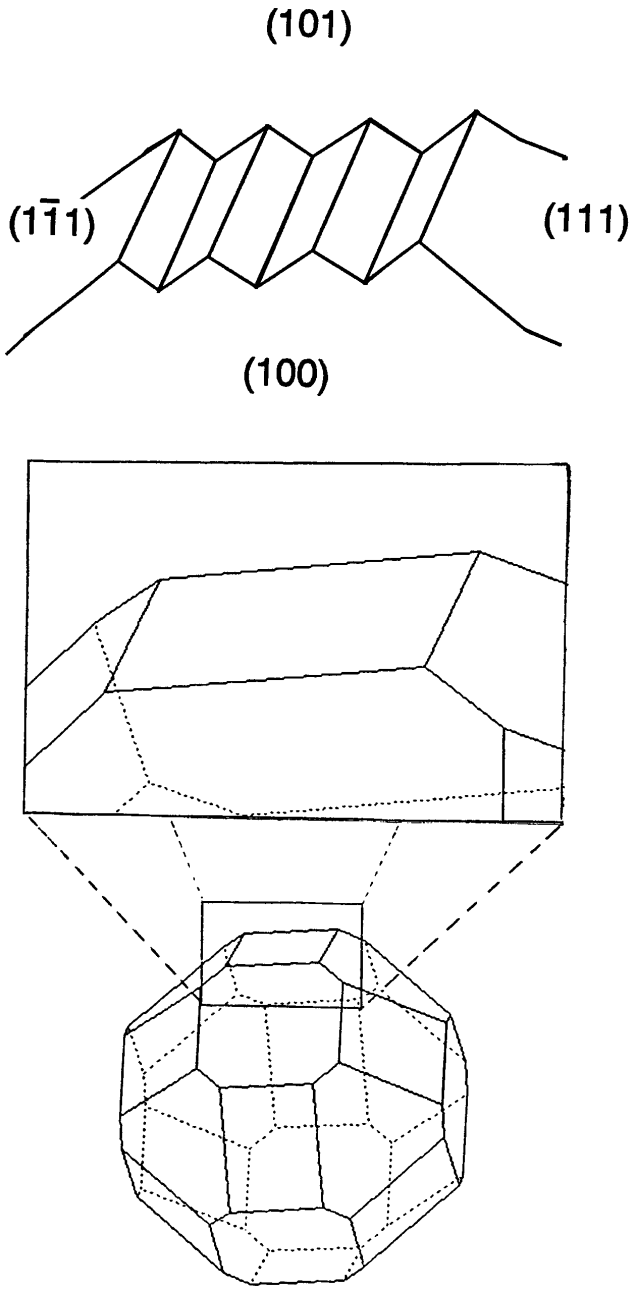

FIG. 3. The {110} facets were actually decomposed into a hill-and-valley structure composed of two sets of small {111} facets with 109.5° interangle. The surface geometry of the enlarged rectangle face, (101), is shown.

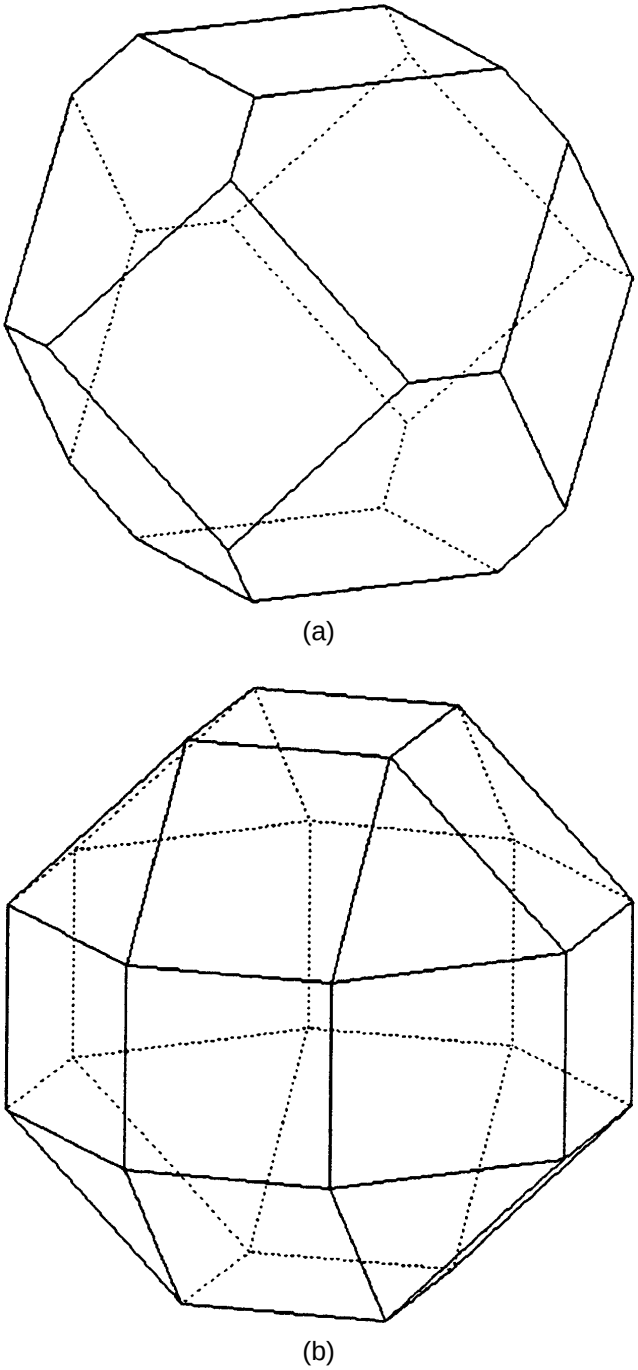

FIG. 4. The {110} area varies from zero (a) to the maximum (b) when it impinges on another {110}. In (a), the {110} area factor V is zero (no {110}, $L = L_0$), while in (b) V is 0.5 (maximum {110}, $L = 0$). Both figures were captured from the computer screen in 3D graphic mode. (See text for the definition of V.)

particles from TEM micrographs, by the help of program 3D, we found that most particle shapes varied in a very small range, $GR = 0.98–1.01$ and $V = 0.35–0.40$.

III. PROGRAM 3D

A. General information

The program was written in Turbo Pascal 5.5 for IBM or compatible PC 286 and higher computers. Because of the large size and complexity of the program, it would be inappropriate to try to delineate the programming or to give a detailed user guide. For more information please contact the authors.

The following four assumptions were made:

(i) The particles are single crystals of cubic symmetry. Another version of 3D can handle particles with other crystallographic systems, but in this study only the cubic system is considered.

(ii) The particles have reached the equilibrium shape. The energy ratio (*GR*) can be adequate only when the Wulff construction is valid. This also implies that twins, stacking faults, or other defects are absent.

(iii) Only {100}, {111}, and {110} facets exist.

(iv) The hill-and-valley structure of {110} was ignored and those facets were treated as flat facets.

B. An example

The operating procedure of 3D can be demonstrated by a typical example. Figure 5(a) is a TEM micrograph of three sintered particles in a chain. The geometric model [Fig. 5(b)] of these three particles was derived as follows:

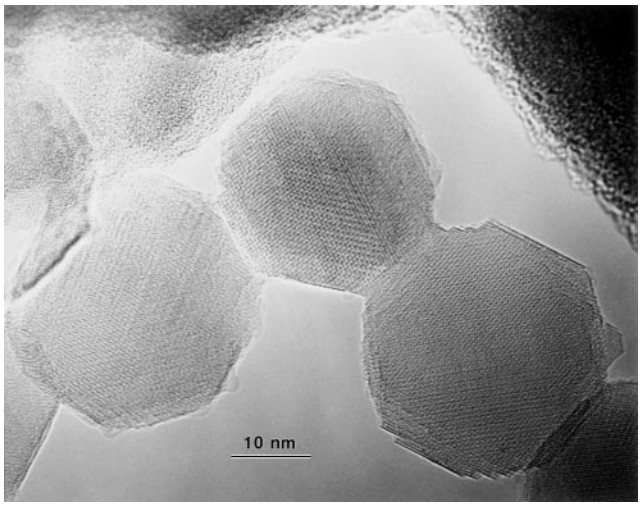

(a)

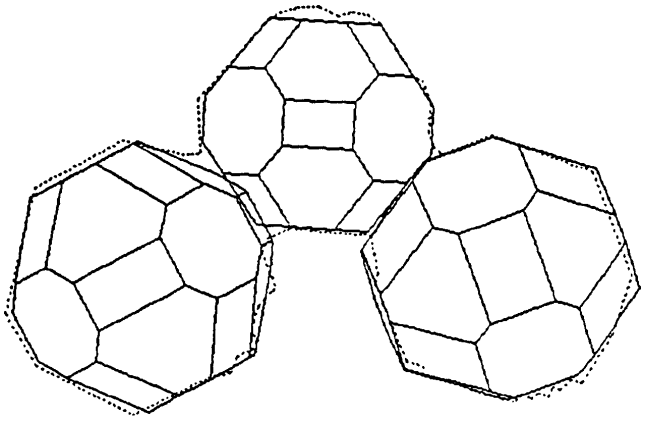

(b)

FIG. 5. (a) TEM micrograph of three sintered particles in a chain (courtesy J. E. Bonevich). (b) A 3D geometric model of above three particles. The broken lines were traced from the micrograph, and solid lines were generated by 3D.

(i) A digitizer was used to record the coordinates (*X* and *Y*) of a series of points which best describe the outline of the particles by connecting the points with straight lines. The coordinate data were saved in a 3D recognizable file format (template). The file can be loaded into 3D and shown on the computer screen [Fig. 6(a)].

(ii) 3D was started and three particles were defined.

(iii) The template file was loaded and shown on the screen along with the particles defined in step 2 [Fig. 6(b)].

(iv) Each particle is moved to its probable position [Fig. 6(c)].

(v) The size, shape, and orientation of one particle are adjusted by trial and error to match the template outline. The shape is changed by altering its energy ratio (*GR*) and {110} area parameter (*V*) [Fig. 6(d)].

(vi) Step 5 is repeated for the other two particles [Fig. 6(e)]. Now we have a 2D model that can adequately fit the template.

(vii) In steps 5 and 6, the particles are adjusted only in *y* and *z* directions (the page surface) to match the template outline, and there is no information about *x* direction (vertical to the page). That is, the simulated particles may not contact with each other if we see them in 3D. Because we know in reality that these particles do make contact, we need to adjust the position of each particle in the *x* direction until they contact each other. (This adjusting procedure can be done easily by viewing from the side of the chain.) The geometric relationship in 3D can now be viewed in any desired direction by rotation. Figure 6(f) shows one such view of the contact between two particles.

C. Characteristics

3D provides a routine method to find geometric shapes of particles by interactively responding to user's commands in graphic mode. Since the result of each command (whether it is a rotation, translation, magnification, zooming, or shape changing command) can be observed on the screen immediately, the matching procedure is rapid. The program can describe particle shapes over the entire range shown in Fig. 7.

D. Results

After examining several hundred micrographs, we found no noticeable shrinkage in these sintered alumina particle pairs. This clearly indicated that surface diffusion was the predominant sintering mechanism which formed the necks. Although volume diffusion from surface to neck and evaporation-deposition could also create

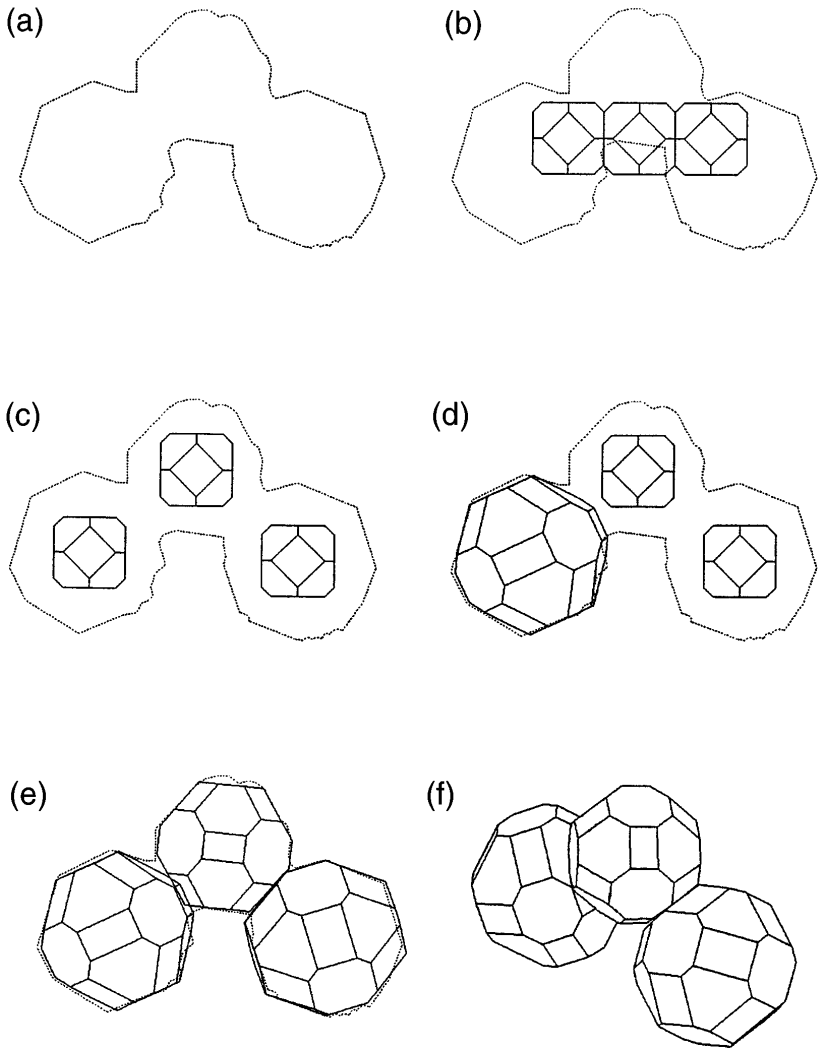

FIG. 6. (a–f) The 3D operating procedure (see text).

the same results, volume diffusion is expected to be too slow compared to surface diffusion, and the vapor pressure of alumina is sufficiently low at the sintering temperature that evaporation-condensation should not be a major factor.

IV. PROGRAM BUMP

A. General information

This program is an extension of 3D and was written in Turbo Pascal 6.0 for IBM or compatible PC 286 and higher computers.

BUMP was intended to determine whether the observed particle chains were created by chance, or did rearrangement occur after initial contact. Comparing TEM micrographs of sintered and nonsintered particle chains, we found little difference in either particle shape or in their geometric arrangement. Thus, rearrangement to a stable configuration must have occurred immediately after any particle contacted another. It is reasonable to expect initial particle contact to be random, with the exception of magnetic material chains.[33–35] The program BUMP was written to document random contacts, enabling comparisons with observed particle to particle relationships.

B. Six possible contact conditions

A typical alumina particle possesses 6 {100} facets, 8 {111} facets, 12 {110} facets, 72 edges (three types: edges between {100} and {111}, {111} and {110}, and {100} and {110}), and 48 corners. Although BUMP can distinguish these complicated contact conditions with little difficulty, it would be hard to make a meaningful comparison due to the complexity. Therefore, we considered only three elements: face, edge, and corner, and thus only six possible contact conditions, as shown in Fig. 8.

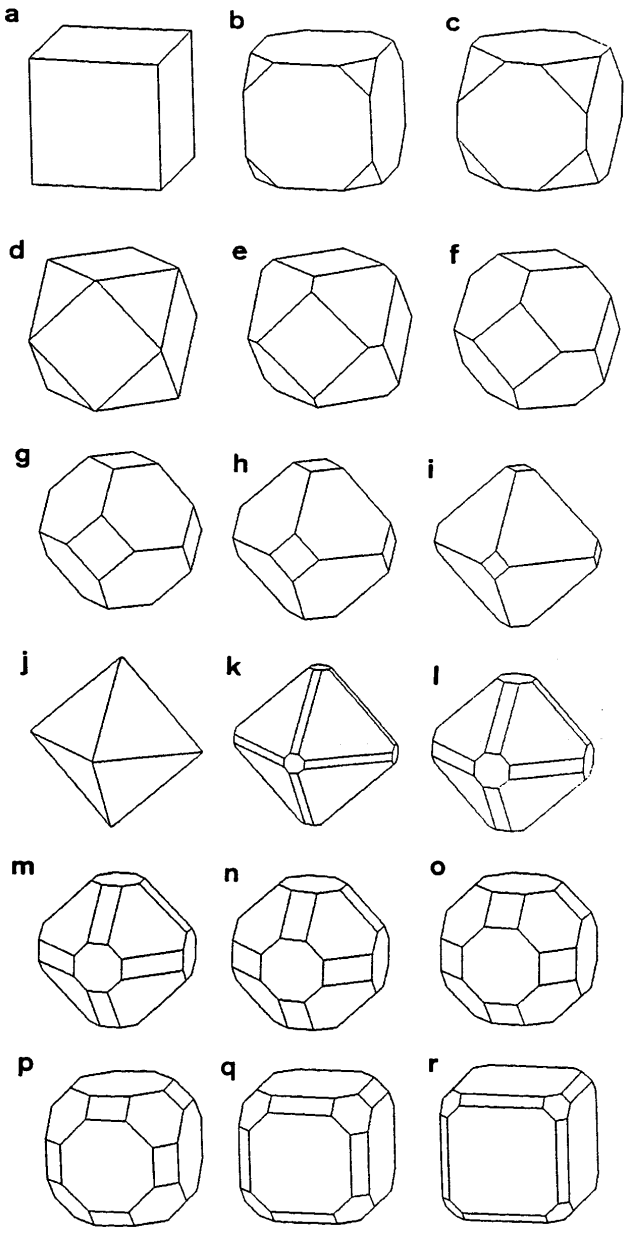

FIG. 7. (a–r) Ten views of a cuboctahedron with addition of {110} facets in various orientations. Each shape has 26 faces: 6 {100} (octagon), 8 {111} (hexagon), and 12 {110} (rectangle). This figure was generated by computer program 3D.

C. Simulation algorithm

The results of BUMP were obtained as the relative frequency of occurrence of each of the above six contact conditions. In each run two particles were brought together until they touched in one of the six contacts. Figure 9 demonstrates the procedure of each simulation. First, a predefined particle sits at the origin with fixed shape and orientation [Fig. 9(a)]. Second, the other particle is randomly oriented and put into a random position in space (b). Third, the second particle moves along the line connecting the two particle centers to the farthest possible contact position, i.e., imagining that each particle is enclosed within a sphere, and bringing them closer until the two spheres touch (c). Fourth, the second particle is brought closer to the first one gradually until they touch (d). The typical approach distance of each step was 0.001 nm.

Several assumptions were made in writing this program. First, the center-to-center approach of two particles could adequately include all possible contacts with correct probabilities. Second, the hill-and-valley structure of {110} could be treated as flat facets. Since the height difference of the {110} hill-and-valley structure was on the order of one nanometer, one does not expect any significant error. Third, edge-to-face and face-to-face elements were considered as contacting if the interangle between them was less than two degrees. A typical length of a face or edge for a 20 nm diameter particle was about 6 nm. Considering two 6 nm lines as the two sides of a triangle, where the third side has the length of an atom (about 0.2 nm), the interangle between the lines is about two degrees. Therefore, an interangle less than two degrees meant no atom could fill in the space. In other words, the two elements were in contact. Fourth, if the distance between a corner and another element was less than 0.2 nm, then it was counted as a corner contact.

On a few occasions the contact fits into more than one type of contact (Fig. 8). Two subgroups could be found. The first was contact (1), (3), (5), and (6), and the second was contact (1), (2), (4), and (5). We assigned the order of priority as (6) $>$ (5) $>$ (1) $>$ (3) for the first subgroup, and (5) $>$ (2) $>$ (1) $>$ (4) for the second. For example, if a contact is face-to-face (6), it is also edge-to-face, type (5), since the edge is part of the face; the contact was counted as face-to-face.

BUMP shared a large portion of the code of 3D, so it could simulate particles of a wide range of shapes and sizes. Although it was not written for graphic mode, the output could be recorded and loaded into 3D for observation.

To confirm the correctness of the program, we loaded all eleven face-to-face contacts in one test simulation (3000 runs) into 3D, and observed that they were indeed face-to-face contacts. None of the eleven face-to-face contacts was fully overlapped.

D. Results

A typical simulation result is shown in Table I, where two 20 nm particles were brought together 10,000 times. Comparing this simulation to experimental results, we noticed two things that were significantly different. First, face-to-face contact was only 0.62% in the simulation, while about 80% of nonconstrained particles (not constrained by other particles in chains) and more than

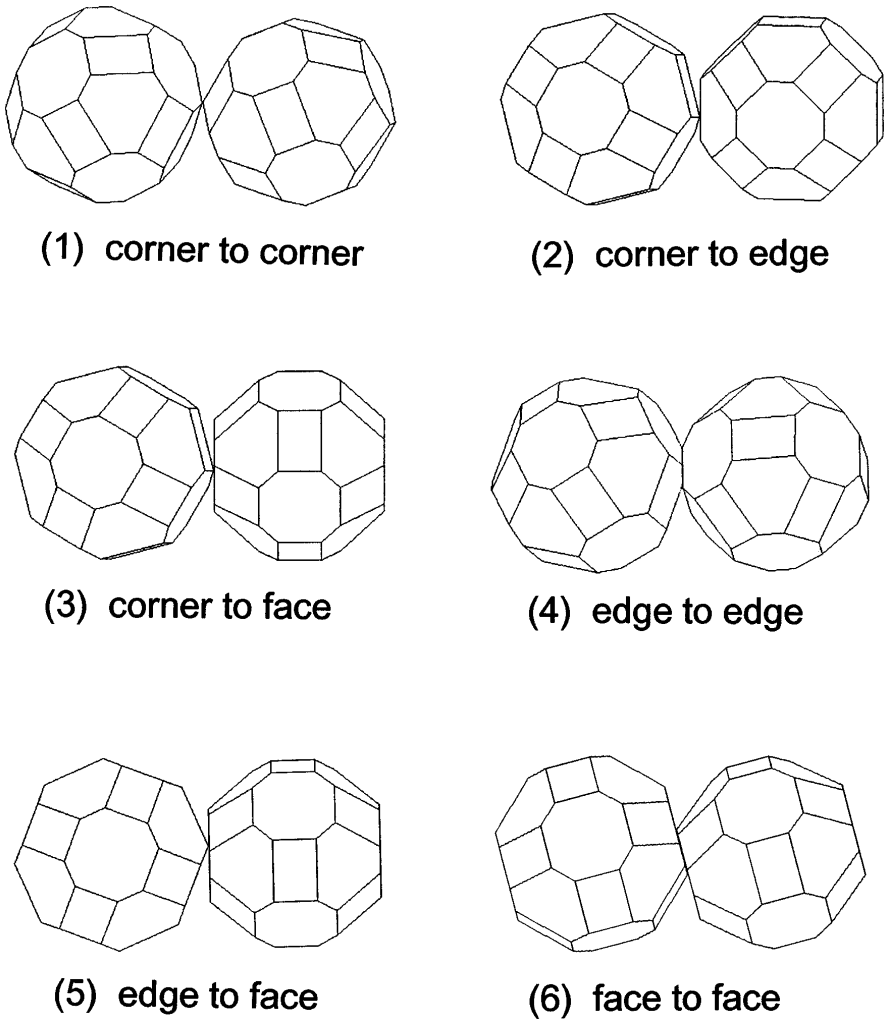

FIG. 8. Six possible contact conditions of two alumina particles with typical shape. Only three elements—corner, edge, and face—were considered.

half of constrained particles were face to face or very nearly so. Second, in the simulation only a few had good particle alignment, while experimentally at least 60% of the particles had good alignment.

The simulation confirmed that the probability of face-to-face contact was small, and the probability for full overlap was smaller still. The most probable contacts, corner-to-face and edge-to-edge, each with about 36% probability, were hardly even found in the micrographs. Consequently, the usual fully overlapped face-to-face contacts led to the conclusion that there must have been rotation and sliding of one particle with respect to the other after or just before contact was made. When the particles contacted by chance, the three most probable contact conditions, namely, corner-to-face, edge-to-edge, and edge-to-face, might rotate into more stable positions to reduce the total surface energies, for instance, into a partial face-to-face contact. If they had enough energy to overcome the energy barrier, the partially contacting faces can increase the contact area by sliding. Since our particles were of ultrafine size, the whole process may proceed extremely fast.

TABLE I. One typical result for two 20 nm particles for 10,000 runs.

No.	Contact conditions	Times	Percent (%)
(1)	Corner-to-corner	10	0.10
(2)	Corner-to-edge	323	3.23
(3)	Corner-to-face	3558	35.58
(4)	Edge-to-edge	3609	36.09
(5)	Edge-to-face	2438	24.38
(6)	Face-to-face	62	0.62

V. CONCLUSION

Two computer programs, 3D and BUMP, were developed to help interpret the micrographic results and

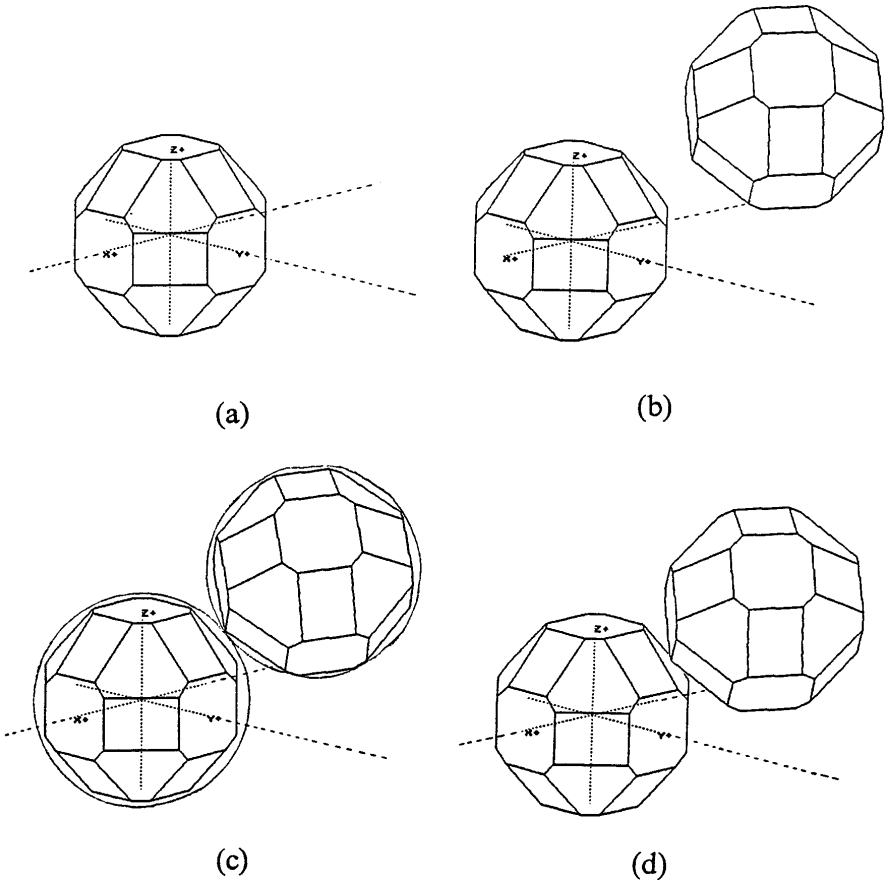

FIG. 9. (a–d) The simulation procedure of BUMP (see text).

solved two specific problems. 3D showed that the sintered ultrafine alumina particle pairs had no shrinkage; therefore, surface diffusion was the predominant sintering mechanism. BUMP showed that the original particle chains before sintering were not formed purely by chance contact. Instead, rotation and sliding brought the particles into nearly fully overlapping face-to-face contact.

ACKNOWLEDGMENTS

This work was supported by the U.S. Department of Energy, Contract No. DE-FG02-87ER45309, and Materials Science and Engineering Department, Northwestern University.

REFERENCES

1. G. C. Kuczynski, Trans. Am. Inst. Min. (Metall.) Eng. **185**, 169 (1949).
2. C. Herring, in *The Physics of Powder Metallurgy*, edited by W. E. Kingston (McGraw-Hill Book Co. Inc., Reading, MA, 1951), Chap. 8, p. 143.
3. C. Herring, in *Structure and Properties of Solid Surfaces*, edited by R. Gomer and C. S. Smith (University of Chicago, Chicago, 1953), Chap. I, p. 5.
4. W. D. Kingery and M. Berg, J. Appl. Phys. **26**, 1205 (1955).
5. W. W. Mullins, J. Appl. Phys. **28**, 333 (1957).
6. R. L. Coble, J. Am. Ceram. Soc. **41**, 55 (1958).
7. R. L. Coble, J. Appl. Phys. **32**, 787 (1961).
8. R. L. Coble, J. Appl. Phys. **32**, 793 (1961).
9. R. L. Coble, J. Appl. Phys. **41**, 4798 (1970).
10. A. E. Paladino and R. L. Coble, J. Am. Ceram. Soc. **46**, 133 (1963).
11. F. A. Nichols and W. W. Mullin, J. Appl. Phys. **36**, 1826 (1965).
12. F. A. Nichols, J. Appl. Phys. **37**, 2805 (1966).
13. R. L. Coble and T. K. Gupta, in *Sintering and Related Phenomena*, edited by G. C. Kuczynski, N. A. Hooten, and C. F. Gibbon (1967), p. 423.
14. D. L. Johnson, J. Appl. Phys. **40**, 192 (1969).
15. D. L. Johnson, J. Am. Ceram. Soc. **53**, 574 (1970).
16. R. L. Coble and R. M. Cannon, Mater. Sci. Res. **11**, 151 (1978).
17. W. S. Coblenz, J. M. Dynys, R. M. Cannon, and R. L. Coble, in *Sintering Processes*, edited by G. C. Kuczynski (Materials Science Research **13**, Plenum Press, New York, 1980), p. 141.
18. J. E. Bonevich, Ph.D. dissertation, Northwestern University, Evanston, IL (1991).
19. J. E. Bonevich, M. H. Teng, D. L. Johnson, and L. D. Marks, Rev. Sci. Instrum. **62**, 3061 (1991).
20. M. H. Teng, Ph.D. dissertation, Northwestern University, Evanston, IL (1992).
21. J. E. Bonevich and L. D. Marks, J. Mater. Res. **7**, 1489 (1992).
22. M. H. Teng, J. E. Bonevich, L. D. Marks, and D. L. Johnson, unpublished.
23. S. Iijima, Jpn. J. Appl. Phys. **23**, L347 (1984).
24. S. Iijima, J. Elec. Micro. **34**, 249 (1985).

25. C. E. Warble, J. Mater. Sci. **20**, 2512 (1985).
26. T. Hirayama, J. Am. Ceram. Soc. **70**, C122 (1987).
27. J. E. Bonevich, in *Proceedings of the 47th Annual Meeting of the Electron Microscopy Society of America*, edited by G. W. Bailey (San Francisco Press, San Francisco, CA, 1989), p. 258.
28. C. Kaito, K. Fujita, H. Shibahara, and M. Shiojiri, Jpn. J. Appl. Phys. **16**, 697 (1977).
29. J. W. Gibbs, *The Collected Works, Vol. 1, Thermodynamics* (Longmans, New York, 1931), p. 320.
30. P. Curie, Bull. Soc. Mineral. Fr. **8**, 145 (1885).
31. G. Wulff, Z. Kristallogr. **34**, 449 (1901).
32. C. Herring, Phys. Rev. **82**, 87 (1951).
33. K. Kimoto, Y. Kamiya, M. Nonoyama, and R. Uyeda, Jpn. J. Appl. Phys. **2**, 702 (1963).
34. A. R. Thölén, Acta Metall. **27**, 1765 (1979).
35. A. R. Thölén, Physica Scripta **37**, 231 (1988).